Electronically transparent Ag-C(sp^3) contacts result in low conductance junctions

Thomas M. Czyszczon-Burton,[a,†] Enrique Montes,[b,†] Jazmine Prana,[a] Sawyer Lazar,[a] Nils Rotthowe,[a] Sully F. Chen,[a] Héctor Vázquez,[b,*] and Michael S. Inkpen[a,*]

[a]*Department of Chemistry, University of Southern California, Los Angeles, CA 90089, USA*

[b]*Institute of Physics, Czech Academy of Sciences, Cukrovarnická 10, Prague 16200, Czech Republic*

E-mail: vazquez@fzu.cz, inkpen@usc.edu

† T.M.C.-B. and E.M. contributed equally to this work.

ABSTRACT

Chemical groups capable of connecting molecules physically and electrically between electrodes are of critical importance in molecular-scale electronics, influencing junction conductance, variability, and function. While the development of such linkage chemistries has focused on interactions at gold, the distinct reactivity and electronic structure of other electrode metals provides underexplored opportunities to characterize and exploit new binding motifs. In this work we show that α,ω-alkanedibromides spontaneously form well-defined junctions using silver, but not gold, electrodes. Through application of the glovebox-based scanning tunneling microscope-based break junction method, we find that the same junctions form when using different halide, or trimethyltin, terminal groups, suggestive of an electronically transparent silver-carbon(sp^3) contact chemistry. However, the conductance of these junctions is ~30× lower than for analogous junctions formed on gold and does not align with predictions based on first-principles calculations. Through insights provided from prior temperature-programmed desorption studies and a robust series of atomistic simulations and control experiments, we propose that in these experiments we measure alkoxide-terminated junctions formed through the reaction of unstable silver-alkyl species with adsorbed surface oxygen. This study, in demonstrating that high conductance contact chemistries established using model gold electrodes may not be readily transferred to other metals, underscores the need to directly characterize the interfacial electronic properties and reactivity of electrode metals of wider technological relevance.

KEYWORDS

single-molecule junctions, silver electrodes, surface-mediated reactions, transport calculations, glovebox-based scanning tunneling microscopy

INTRODUCTION

Inspired by the established chemistry of self-assembled monolayers,[1] the first reported single-molecule junctions comprised gold electrodes bridged by thiol-functionalized organic compounds.[2,3] A wide variety of linker groups have since been identified to be compatible with gold,[4] and a subset of these have been found to form junctions with other metal electrodes. For example, room temperature scanning tunneling microscope-based break junction (STM-BJ) studies with silver electrodes have utilized aurophilic thiol (-SH),[5] nitrile (-CN),[6,7] amine (-NH_2),[5–10] pyridyl (-C_5H_4N),[11,12] alkyne (-CCH),[13–15] and carboxylic acid (-COOH)[16–18] linkers. The chemical properties of such groups are known to impact junction properties in several important ways, exerting a strong influence over the conducting orbital level alignment and electronic coupling,[4,9,19–23] junction mechanical stability,[24,25] or even imparting conductance switching functionality.[26,27]

While different electrode metals exhibit distinct surface structures, electronic properties, and intrinsic reactivities, the ability of a chemical group to function as a linker on some metals but not others is widely underexplored. We are only aware of one study by Jo *et al.* who report that methoxy (−OMe) groups, which do not bind to gold, are capable of forming junctions with silver leads.[28] The discovery and development of non-gold contact chemistries has clear potential to drive significant advances in molecular electronics and surface assembly, for example, by establishing distinct metal-molecule bonding interactions with useful mechanical or electronic character, or enabling the *selective* self-assembly of molecules on mixed metal substrates. More broadly, the identification of appropriate contact chemistries to form molecular junctions with less diffusive electrode metals than gold may prove critical to establishing the utility of prospective hybrid molecule-semiconductor integrated circuitry.[29] Studies of single-molecule junctions that expose new interfacial chemical transformations[30] could also provide important insights into reaction discovery and development in on-surface chemistry,[31] as well as studies of heterogeneous catalytic chemical processes.[32]

Electrode linker groups are commonly incorporated into organic molecules via synthetic routes that start from halide (X)-functionalized precursors (particularly for X = Br and I). Such precursors are commercially ubiquitous due to their utility in a wide range of chemical transformations, and the distinct rates of reactivity of C−X bonds which enable modular, multistep reaction strategies. These factors also contribute to growing interest in the *direct* use of halides as electrode linkers. This approach could not only significantly reduce the number of synthetic steps required to prepare molecular junction components, but also enable

the characterization of systems in which the incorporation of conventional contact groups is challenging. With gold electrodes, it has been reported that junctions can be formed using thiophenyl-,[33] alkyl-[34] and aryl-iodides,[35–38] as well as halide-capped clusters.[39] Depending on the experimental conditions, such junctions are proposed to comprise either physisorbed Au-X (coordinating through the halogen lone pairs) or chemisorbed Au-C contacts (following oxidative addition of C-I), although their exact contact chemistry has not always been determined unambiguously.

The use of organohalides to directly form chemisorbed Au-C contacts is an attractive proposition, avoiding established precursors with toxic -$SnMe_3$ groups or laborious preinstallation of Au-C bonds.[23] These linkages are among the most electronically transparent contacts for single-molecule junctions, due to Au-C "gateway" states that are well coupled to both the electrode and the molecular backbone.[23,40] Although aryl iodides are typically considered among the most reactive of the organohalides, exhibiting faster rates of oxidative addition than arylbromides, arylchlorides, or alkyl halides,[41–43] their use to form gold-aryl linked junctions *in situ* at room temperature has so far been demonstrated only through the application of reducing potentials in an electrochemical environment,[36] or exposure to atomically rough surfaces in polar solvents that generate a large interfacial electric field.[37,44] Despite the increased reactivity of non-gold metals towards activation of C-X bonds relative to gold,[45,46] the application of these electrode materials to form molecular junctions from organohalides has not yet been reported. Indeed, the only non-gold metal-carbon (M-C) contacts probed in single-molecule junctions are Ag-C(sp) linkages formed from terminal alkynes,[13–15] or M-C(sp^2) contacts formed *in situ* from N-heterocyclic carbene precursors (M = Ag, Cu),[47] leaving their properties broadly underexplored.

In this work we show, through application of the glovebox STM-BJ method, that simple bromide-terminated alkanes, **CnBr** (n = 4-12), form well-defined single-molecule junctions with silver electrodes under an inert nitrogen atmosphere (**Figure 1**, top). Remarkably, these junctions form spontaneously from non-polar solutions at room temperature, even at low tip-substrate bias (10 mV). To establish the nature of the interfacial contact, we performed a robust series of control experiments and first-principles transmission calculations based on density functional theory (DFT). Measurements of **C8X** (X = -I, -Cl, or -$SnMe_3$) produced near-identical conductance features to those of **C8Br**, indicating that each of these compounds are precursors that react *in situ* to produce junctions of similar geometry. Notably, the observed peak features occur at an unusually low conductance: ~30× lower than Au-C(sp^3) linked junctions of the same alkane length,[23] and 2.5× lower than for analogous Ag-S linked junctions

which comprise two additional S atoms in the molecular backbone (**Figure 3a**). Transmission calculations further show that alkane junctions linked by Ag-C contacts should be slightly *more* – not significantly less – conducting than their Au-C linked analogues (**Figure 3b**), together establishing that we do not measure chemisorbed Ag-C(sp^3) linked alkane junctions in these experiments. Drawing insights from prior surface science studies,[48–51] we propose instead that while Ag-C(sp^3) linked junctions do initially form from **C8X** precursors, they subsequently react with surface-adsorbed oxygen (noting that O_2 is present in ppm quantities) to form silver-alkoxides that we trap and measure in molecular junctions (**Figure 1**, bottom). This hypothesis is supported here by transmission calculations which show Ag-O-alkyl terminated junctions exhibit conductance values consistent with the features we observe experimentally, and additional control experiments that rule out other plausible secondary processes such as α- or β-hydride elimination reactions.

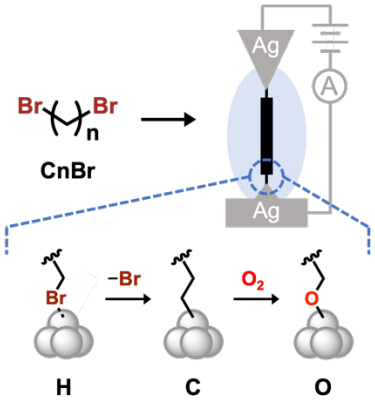

Figure 1. A schematic showing a single-molecule junction formed using silver electrodes from solutions of α,ω-dibromoalkanes (**CnBr**) under an inert nitrogen atmosphere inside a glovebox. *Bottom:* **CnBr** precursors can feasibly interact with the electrode surface in different ways, forming alkyl halide- (H), alkyl- (C), or alkoxide-contacted (O) junctions following loss of the halide and reaction with surface-adsorbed oxygen.

RESULTS AND DISCUSSION

We perform conductance measurements with silver electrodes using a STM-BJ setup housed inside an inert atmosphere glovebox that has been described previously (see **SI** for more details).[52,53] To remove the majority of native oxide from oxyphilic silver surfaces, we mechanically cut tip wire and polish an evaporation slug substrate inside the glovebox. Following this, STM-BJ measurements are performed by applying a voltage bias (V) across the tip and substrate while measuring the current (I), converted to conductance G (= I/V), as

the electrodes are pushed in and out of contact. In each conductance-displacement measurement, the initially formed large area junction thins to a single-atom contact with increasing tip-substrate displacement, before breaking to form a nanoscale gap between undercoordinated silver atoms. We repeat these measurements thousands of times whereby the resulting traces are compiled, without data selection, into one- and two-dimensional (1D and 2D) conductance histograms.

During experiments under nitrogen or in an anhydrous solvent environment under nitrogen, we observe steps in individual conductance-displacement traces close to 1 G_0 (= $2e^2/h$ = 7.75×10^{-5} S), characteristic of the formation of silver atomic point contacts, which combine to form peaks in the histograms (**SI, Figure S1**). We find the conductance steps for silver atom contacts are typically shorter than the corresponding steps observed using gold electrodes, in agreement with previous work[54] and consistent with reports that atomic chains form more readily with gold than silver.[55] While STM-BJ studies using silver electrodes exposed to air have reported an additional conductance feature close to ~0.1 G_0 that is attributed to the formation of Ag-O-Ag junctions,[9,56] this feature is not typically pronounced in the glovebox-based studies presented here. As evidenced below, additional conductance features are observed below 1 G_0 in the presence of molecules in solution that can bridge the nanogap-separated silver electrodes. Importantly, we find our inert atmosphere glovebox STM-BJ approach can facilitate conductance measurements of molecular junctions formed using silver electrodes at ambient temperature and pressure over extended periods (hours or days) without significant reoxidation of the electrode surface.

In **Figure 2a** we plot overlaid conductance histograms obtained from measurements of 0.1 mM solutions of α,ω-dibromoalkanes (**CnBr**, where "n" represents the number of backbone methylene groups) in tetradecane (TD). In each case we identify a prominent feature (black dotted arrow, **Figure 2a**), with a shoulder or peak of lower intensity at ~2× the primary peak conductance. We attribute these features to 1 and 2 molecule junctions formed from **CnBr**, respectively (**SI, Figure S2**).[57–59] In **Figure 2b** we plot representative traces for **CnBr** measurements (n = 6-12), showing that the step length corresponding to these junctions increases with the number of carbon atoms in the backbone (see **SI, Figure S3** for 2D histograms). The strong correlation between step and molecular length further supports the assignment of these features to molecular junctions formed from **CnBr**. In contrast to an earlier report,[34] our attempts to form molecular junctions with **C8X** solutions (X = Br, I) using gold electrodes provide no clear conductance peak features (**SI, Figure S4**). This shows that **CnX**

do not readily form molecular junctions with gold and implicates a distinct haloalkane-Ag interfacial chemistry.

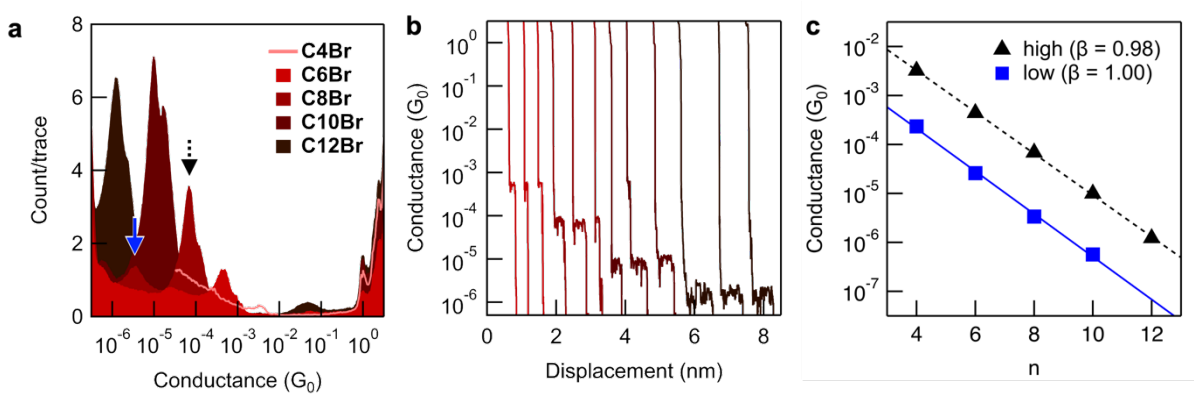

Figure 2. (a) Overlaid 1D histograms obtained from scanning tunneling microscope-based break junction (STM-BJ) measurements of 0.1 mM **CnBr** solutions in tetradecane at 750 mV bias (n = 4-12). Histograms are constructed from 6,000-10,000 consecutively measured traces without data selection. Arrows indicate assigned high (black dotted) and low (blue solid) conductance peaks for **C8Br**. The histogram for **C4Br** is truncated for clarity. Corresponding 2D conductance-displacement histograms are provided in the **SI, Figure S3**. **(b)** Sample conductance-displacement traces for selected junctions (n = 6-12), offset along the displacement axis for clarity. **(c)** A plot of conductance versus number of repeat methylene units (n) for high (black triangles) and low (blue squares) conductance peaks. Exponential fits to each data series using $G = G_c\exp(-\beta n)$ gives $\beta_{(high)} = 0.98/n$, $\beta_{(low)} = 1.00/n$, $G_{c(high)} = 1.6 \times 10^{-1}$ G_0, and $G_{c(low)} = 1.2 \times 10^{-2}$ G_0.

When probing shorter **CnBr** junctions (n = 4-10), we also observe an additional, lower conductance peak feature of reduced intensity (blue solid arrow, **Figure 2a**). This peak typically arises from a step that occurs *after* breaking of the high conductance junctions, as illustrated by the example traces shown in **SI, Figure S5** and in 2D histograms which show regions of reduced counts for displacements prior to the onset of the low conductance feature (**SI, Figure S3**, **S8h**, and **S11c**). Accordingly, we suggest that this feature results from a geometrical rearrangement of the electrode and/or or the molecule during junction displacement that changes the molecule-electrode coupling or frontier orbital energy alignment. The origin of this component appears distinct from that of a similar feature observed for covalent Au-C junctions, which was in that case attributed to a *periodic* electrode deformation that resulted in intermittent jumps to a low conductance geometry with junction elongation.[23] Related conductance features have also been observed in some studies of alkanedithiols measured using gold electrodes, attributed to the formation of $Au(SR)_2$ interfacial contacts.[60]

In **Figure 2c** we plot conductance versus molecular length for each series of peaks, using the most probable values of junction conductance obtained from Gaussian fits to histogram peaks (**SI, Table S1**). The conductance of both series exhibits an exponential length dependance, indicative of through-molecule tunneling transport. Tunneling decay constants ($\beta \sim 1/n$), obtained through fits to each series using $G = G_c\exp(-\beta n)$ (where G_c is the contact conductance), agree with previously observed values obtained for junctions with alkane backbones measured on gold or silver.[24,54] However, the nature of the molecule-electrode contact formed from **CnBr** in the primary series remains unclear. Based on earlier studies of halide-terminated molecules on gold (discussed above), instead of a single dominant peak we might expect to observe three peak features associated with junction geometries comprising two chemisorbed Ag-C(sp^3) linkages (**CC**), two physisorbed halogen-bonded Ag-Br interactions (**HH**), or one of each type of contact (**HC**; **Figure 1**).

We first consider the possibility that the dominant peaks from **CnBr** measurements correspond to **CC**-type junctions. If this was the case these junctions would exhibit a surprisingly low conductance, ~30× smaller than reported values for the corresponding gold-alkane-gold junctions formed from trialkylstannyl precursors (**SI, Table S1** and **Figure S6**).[23] To further illustrate this point we present, in **Figure 3a**, overlaid conductance histograms from measurements of 1,10-bis(methylthio)decane (**C10SMe**), **C10Br**, and 1,10-decanedithiol (**C10SH**). This comparison shows that the conductance of **C10Br** junctions is intermediate between junctions comprising physisorbed and chemisorbed sulfur linkers. It is particularly notable that the conductance of **C10SH** junctions, comprising two additional sulfur atoms compared to **CC**-type junctions formed from **C10Br**, are 2.5× higher. With gold electrodes the opposite trend is found, as junctions formed from **C8SH** are ~22× *lower* in conductance than the Au-C(sp^3) linked gold-octane-gold analogue.[23,61] Remarkably, conductance histograms of **C4Br** and **C6Br** comprise no substantial secondary features that align with the primary conductance peaks obtained from studies of **C8Br** and **C12Br** (**Figure 2a**). If these junctions had a **CC** geometry, this would appear to indicate that the rate of formation of dimers via C-C homocoupling reactions on silver electrodes is significantly slower than with gold electrodes, as dimers are commonly observed in studies of Au-C linked junctions.[23,36,37] This contrasts with expectations based on the results of temperature programmed desorption (TPD) experiments, where silver is reportedly unique in mediating alkyl homocoupling reactions at temperatures >190 K relative to other decomposition pathways.[62,63] Accordingly, the silver-alkyl motif is expected to exhibit a high reactivity at room temperature, as further illustrated through unsuccessful attempts to isolate related molecular complexes.[64] In contrast, analogous

gold-alkyl complexes are readily prepared[65] and have been successfully utilized as controls with pre-installed Au-C bonds to help assess whether Au-C interfacial contacts have formed in molecular junctions.[23]

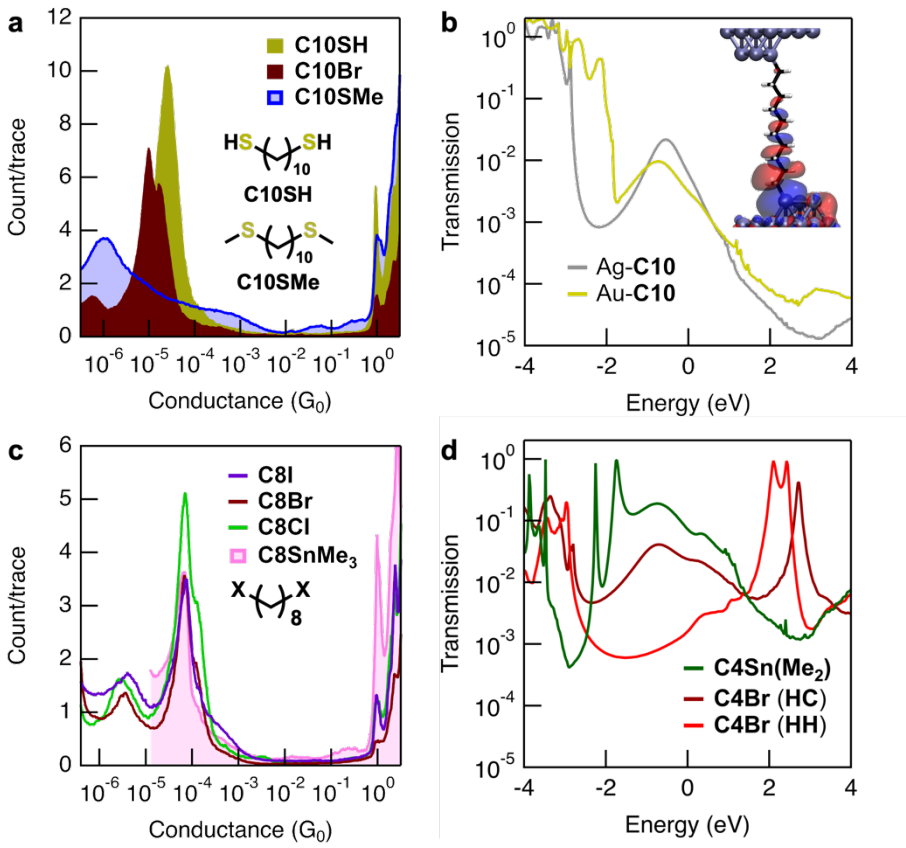

Figure 3. (a) Overlaid 1D histograms from conductance measurements of **C10SMe**, **C10Br** (reproduced from **Figure 1b** for convenience) and **C10SH** with silver electrodes. The conductance of **C10Br** junctions is intermediate between those with sulfur linkers, where **C10SH** junctions exhibit a higher conductance than **C10Br** despite comprising two additional S atoms in the molecular backbone for junctions of the **CC**-type. Histograms were constructed from 6,000-10,000 traces. The corresponding 2D conductance-displacement histograms for **C10SMe** and **C10SH** are shown in the **SI, Figure S7**. **(b)** DFT-based transmission spectra of Ag-**C10** and Au-**C10** (decane-based) junctions, plotted relative to the Fermi level (E_F). *Inset:* scattering state of the Ag-**C10** junction at E = −0.6 eV at the center of the Brillouin zone. **(c)** Overlaid 1D histograms for junctions formed from iodide- (**C8I**, purple), bromide- (**C8Br**, red; reproduced from **Figure 1a** for convenience), chloride- (**C8Cl**, green) and trimethylstannyl-terminated (**C8SnMe$_3$**, pink) 1,8-octane wires (6,800-10,000 traces). **C8I** was measured using a solution concentration of 0.01 mM to facilitate the clean breaking of junctions. **C8SnMe$_3$** was measured using a solution concentration of ~8 mM at 50 mV, after 40 h of solution-substrate contact to maximize peak intensity. While the conductance peak in the presented data for **C8Cl** appears more intense than for the other α,ω-dihalooctanes, peak intensities were found to vary for all analytes from experiment to experiment. Corresponding 2D histograms for **C8X** are shown in the **SI, Figure S8a-d**. **(d)** Calculated transmission spectra of **C4Sn(Me$_2$)** (dark green), **C4Br** (**HC**, dark red), and **C4Br** (**HH**, light red) junctions.

We performed DFT-based transmission calculations of Au-C(sp^3) and Ag-C(sp^3) contacted junctions to help rationalize the surprisingly low conductance of junctions formed

from **CnBr**. In **Figure 3b,** we compare the transmission spectra of **C10** (decane-based) junctions comprising direct, covalent C(sp^3) bonds to Ag or Au electrodes, calculated at the DFT level (with energy plotted relative to the Fermi level ($E_F = 0$)). Remarkably, both spectra are qualitatively similar, exhibiting a broad peak centered at −0.6 eV that derives from electronic states localized at the Au-C and Ag-C bonds. In **Figure 3b**-*inset*, we show the real-space representation of the current-carrying eigenchannel of the Ag-**C10** junction at this energy calculated at the center of the Brillouin zone, which reveals the electrode and backbone states are well coupled through the Ag-C(sp^3) bond. In the **SI, Figure S12**, we present additional transmission calculations of Ag-alkyl junctions with different backbone lengths. These spectra all exhibit qualitatively similar features, comprising a broad transmission resonance close to the Fermi level (E_F) which results in highly conducting junctions (see **Table S3** for selected data). Importantly, our analogue benchmark simulations with gold electrodes are consistent with the previous findings of Cheng *et al.*[23] Across the different backbone lengths, our calculations yield transmission values at E_F that are ~2× higher for Ag-alkyl junctions than for Au-alkyl junctions.

While it is well known that DFT calculations suffer from inherent deficiencies in the calculation of molecular resonance energies, we stress these are unlikely to alter the relative calculated conductance of the Ag- and Au-alkyl junctions studied here. Notably, corrections to these deficiencies based on the DFT+Σ methodology have been devised for weakly-interacting junctions, yet such adjustments may not be appropriate for junctions linked through strongly interacting chemisorbed Ag-C(sp^3) or Au-C(sp^3) contacts. Assuming a rigid translation of the DFT spectra towards lower energies (**Figure 3b** and **SI Figure S12**), large shifts in the Ag-C resonance states (>3 eV) would be needed to achieve the relative conductance values measured here for junctions formed from **CnBr**. While smaller resonance shifts of 1.4-2 eV have been reported for weakly-bonded molecular junctions,[66–68] level corrections might be expected to be even smaller in covalently bonded interfaces.[69,70] Accordingly, the required value of >3 eV for Ag-alkyl covalent bonds appears too high to be reasonable. Furthermore, we cannot physically rationalize why such resonance shifts would be so much larger for Ag-alkyl junctions than for analogue Au-alkyl systems, to reconcile the ~30× lower measured conductance of Ag-alkyl junctions compared to the same junctions formed with gold electrodes. Accordingly, DFT transmission calculations show that the conductance of alkyl junctions with Ag-C(sp^3) linkages should be comparable to, and even slightly higher than with Au-C(sp^3) bonds, and strongly suggest that the **CnBr** junctions measured experimentally do not comprise chemisorbed Ag-C(sp^3) bonds (i.e., they do not have **CC** contact geometries).

We next performed a series of control studies comprising alkanes with different terminal groups to establish whether the junctions formed from **CnBr** have **HC** or **HH** contact geometries. We plot, in **Figure 3c**, overlaid conductance histograms for measurements of **C8X** (X = I, Br, Cl, $SnMe_3$; where **C8SnMe$_3$** was measured as a mixture in a ~1:0.3 molar ratio with 1-trimethylstannyloctane, see **SI, Figures S18-20**) which all show a near identical high conductance feature at 6-7 × 10^{-5} G_0. This finding strongly suggests that the junctions we measure in each case result from the *in situ* cleavage of these terminal groups to form junctions of identical composition and geometry, particularly given that the -$SnMe_3$ group is not expected to form a physisorbed contact. To rigorously evaluate this proposal, we calculate the conductance of model junction geometries comprising terminal groups that interact with silver electrodes through one (**HC**), or two (**HH**), physisorbed Ag-Br or chemisorbed Ag-Sn contacts (**CnSn(Me$_2$)**, feasibly formed through cleavage of a Sn-Me bond).

In **Figure 3d**, we plot overlaid transmission functions for such junction geometries with **C4** (butane-based) backbones. Additional transmission spectra for analogous **HC** and **HH** junctions comprising different alkyl halides are shown in the **SI, Figures S13** and **S14**. The representative spectra shown in **Figure 3d** exhibit transmission peaks at energies characteristic of either the **H** or **C** silver-molecule contact. Spectra of **HC** junctions show a broad peak at −0.7 eV, the signature of the Ag-C resonance which dominates the zero-bias conductance, as well as a peak around 2-3 eV which corresponds to the Ag-halide bond. Spectra of **HH** junctions exhibit two peaks in the unoccupied range of the spectrum (>2 eV) corresponding to both Ag-halide resonances. In contrast, **CnSn(Me$_2$)** junctions comprising Ag-Sn(Me_2) contacts show two peaks below E_F, both derived from the Ag-Sn contact, the broader of which dominates the zero bias conductance. Notably, the calculated conductance of **HC** junctions is >1 order of magnitude, and the conductance of **CnSn(Me$_2$)** junctions is 2-3 orders of magnitude, higher than **HH** junctions (**SI**, **Figure S15** and **Table S6**). Furthermore, simulations of **HC** and **HH** junctions show that junction conductance changes with the identity of the halogen atom. Compared to bromide-terminated **HC** junctions, the calculated conductance is ~15% smaller and ~40% higher for chloride and iodide contacts, respectively (**SI**, **Table S4**). Such perceptual differences are approximately twice as large in **HH** junctions (**SI**, **Table S5**). These calculations corroborate expectations that the conductance of these junctions should exhibit a significant dependence on the identity of the terminal group, contrasting with our experimental results which show the conductance of junctions formed from **C8X** exhibit the same conductance. This further supports the hypothesis that these halide and trimethylstannyl

groups are lost through reaction at the silver surface and are not incorporated into the junctions we measure experimentally.

We highlight additional features of the experiments shown in **Figure 3c** and related control studies that provide important insights. In contrast to studies using **CnBr**, we found **C8I** was more readily measured as a 0.01 mM solution, rather than at a 0.1 mM concentration where it was difficult to repeatedly break tip-substrate point contacts. It also proved challenging to routinely observe conductance peaks in measurements of **C8Cl** at 0.1-1 mM concentrations. These observations are consistent with the expectation that organoiodides (organochlorides) should interact most strongly (weakly),[71] and react at a faster (slower) rate,[46] with metal electrodes, as noted above. While a small peak feature for **C8SnMe$_3$** at 6-7 × 10^{-5} G_0 was observed immediately in conductance measurements after addition of a ~8 mM solution to the silver substrate, this feature was found to increase in intensity after extended solution-substrate contact. Accordingly, the conductance histogram for **C8SnMe$_3$** provided in **Figure 3c** was obtained ~40 h after introduction of solution to help maximize the histogram peak intensity. We note that a similar observation was reported in studies of 1,4-bis(trimethylstannyl)benzene on gold electrodes,[23] in which conductance steps appeared 2-3 h after addition of a 10 mM solution to the substrate (suggesting slow conversion of the Sn-C bond to a M-C interfacial contact). However, in a repeat of this experiment using silver electrodes we have observed peak features of much higher intensity after only ~4 h of solution-substrate contact, which suggest that the precise tip geometry, and/or the substrate roughness and cleanliness, play an important role in the probability of junction formation from this reactive precursor (**SI, Figure S8g,h**). For completeness, we also performed conductance measurements of **C8SnMe$_3$** with gold electrodes (**SI, Figure S8e**). Here we obtained the same high conductance peak feature as previously reported,[23] directly illustrating the stark differences between the conductance of the resulting junctions formed with gold and silver electrodes. Conductance measurements of **C8X** (X = Br, Cl) and **C6Br** at lower applied bias (100 or 10 mV rather than 750 mV) provide histograms with similar conductance features to those obtained at higher bias, showing that large electric fields are not a prerequisite for junction formation (**SI, Figure S9**). Conductance measurements of **C10Br** using a template-stripped silver substrate[72] gave identical conductance features as those observed using mechanically polished silver substrates (**SI, Figure S10**), indicating that the formation of these junctions is not impacted by surface roughness or adventitious contamination during oxide removal.

The studies above show that the conductance features of junctions formed from **CnBr** are not easily attributed to formation of the **CC**, **HC**, or **HH** geometries that might be expected

based on previous molecular conductance studies. To identify alternative plausible contact chemistries for these junctions, we turn to earlier reports that have applied temperature programed desorption (TPD) to probe chemical reactions of alkyl halides on silver surfaces. Alkyliodides have been most extensively studied, and are found to chemisorb on clean Ag(111) and Ag(110) surfaces between 130-190 K, respectively.[49–51] The alkyl fragments (e.g., $C_nH_{(2n+1)}$) subsequently desorb as homocoupled alkanes ($C_{2n}H_{2(2n+1)}$) at temperatures above 190 K without evidence of dehydrogenation, and adsorbed iodide is found to desorb above 700 K.[50,63] In contrast, when both ethyliodide and molecular oxygen are exposed to a Ag(110) surface, additional products including diethylether and ethoxide are formed.[48,49] This is an important observation, as the O_2 content of the nitrogen atmosphere present during our glovebox STM-BJ measurements can increase from <1 ppm to ~5-20 ppm during a typical experiment (monitored using an oxygen analyzer fuel cell). Even for an excellent glovebox atmosphere comprising 0.1 ppm O_2 at ~1 atmosphere, the theoretical dose of O_2 (~80 Langmuir/s) is far greater than those introduced under ultrahigh vacuum to achieve sub-monolayer or saturation coverages.[73,74]

These TPD studies confirm that while the C-X bond of alkyl halides can undergo rapid scission at room temperature to form silver-alkyl species, these groups are inherently unstable and can subsequently react with adsorbed surface oxygen to form alkoxides. We hypothesize that it is these alkoxides (**CnO**) that we trap and measure in molecular junctions (**Figure 1**). The formation of such junctions, comprising an interfacial Ag-O-C(sp^3) contact that is expected to be less conducting than Ag-C(sp^3), would explain the low junction conductance we observe experimentally in measurements of **CnX**. However, we note that the provision of indisputable experimental evidence to confirm this hypothesis poses a significant challenge. Complexes containing pre-installed Ag-C(sp^3) bonds are difficult to isolate (noted above), rendering their utilization as controls here impractical. Excluding carboxylate-contacted junctions which are expected to bind through a distinct coordination geometry,[16–18] we know of no reported methods to form and probe chemisorbed Ag-O linked junctions and only one recent study of Au-O linked junctions – formed through conductance measurements of deprotonated aryl-OH groups.[75] To date, our attempts to form Ag-O junctions directly from the less acidic alkyl-OH precursors have proven unsuccessful.

In lieu of experimental measurements, we evaluate this hypothesis using computational models. We prepare junctions with each end of the alkyl backbone bonded to an oxygen atom on a silver electrode. Our simulations show that oxygen atoms adsorb on the hollow site on top of silver trimers, in agreement with previous findings.[76] In **Figure 4a**, we plot the transmission

function for a **C10O** junction with two such Ag-O-C(sp^3) contacts, calculated at the DFT level. The occupied resonance at −1.5 eV derives from the Ag-O gateway state and dominates the zero-bias conductance as it extends across E_F. We show, in **Figure 4b**, the real-space representation of the current-carrying eigenchannel state calculated at E_F at the center of the Brillouin zone, confirming that the oxygen 2p states are strongly involved in transport through these junctions. Notably, and in remarkable agreement with the trend observed experimentally (**Figure 3a**), the calculated conductance at E_F for this junction geometry lies between the calculated values for thioether- and thiolate-linked junctions on silver electrodes: 4.5×10^{-6} G_0 for **C10SMe**, 1.7×10^{-5} G_0 for **C10O**, and 9.5×10^{-5} G_0 for **C10S** (**SI, Figure S16**). Transport calculations of **CnO** junctions comprising different alkane lengths (n = 4-10; **SI, Figure S17**) further illustrate that the resonance associated with the Ag-O bond is further from E_F and narrower than that associated with Ag-S and Ag-C bonds, yet remains capable of enhancing transmission at E_F relative to junctions comprising Ag-S(Me) contacts. This makes these oxygen-bonded alkyl junctions less conductive than analogous junctions with chemisorbed Ag-S linkers and significantly less transmissive than with Ag-C(sp^3) contacts. While the calculated conductance of **CnO** junctions agrees well with the measured results, falling within a factor of 2 (**SI, Table S7**), DFT values generally overestimate measured conductance. Accordingly, rather than focusing on the exact quantitative values, we propose these calculations strongly support the existence of an Ag-O-C(sp^3) contact chemistry in the junctions formed from **CnBr** and measured experimentally using the STM-BJ method.

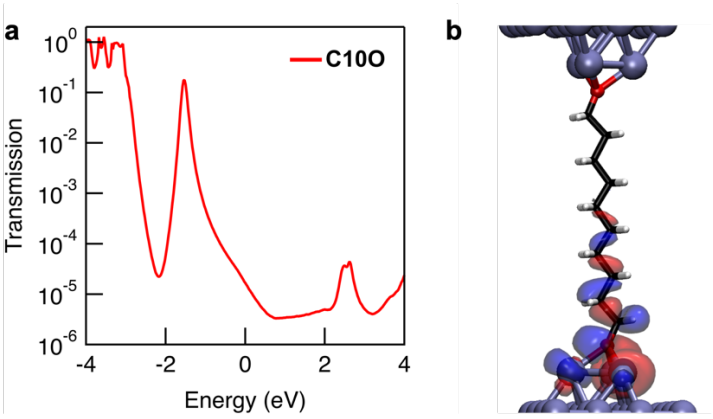

Figure 4. (a) Transmission spectrum of a **C10O** junction, comprising a decane-based backbone with Ag-O-C(sp^3) contacts to both electrodes. **(b)** Transmission eigenchannel calculated at the E_F. Oxygen atoms adsorb on the hollow site of Ag trimer structures.

We perform one final series of conductance measurements to confirm that the junctions formed from **CnBr** do not result from other plausible secondary processes such as α- or β-hydride eliminations. While these chemical reactions have not previously been observed for silver-alkyl species in TPD studies,[51] they have been observed to occur on surfaces functionalized with different metal-alkyl groups[77] and in discreet metal complexes.[78,79] We recognize that such reactions could result in the formation of carbenic, or vinylic π-bound interfacial contacts, respectively (**Figure 5a**). To verify that these contacts do not form we perform a series of control experiments using the compounds shown in **Figure 5b**, in which we have replaced α- and/or β-hydrogens relative to the Br-C (and therefore the projected Ag-C) bond with different groups that have higher bond dissociation energies. This approach follows established strategies in molecular inorganic chemistry that have been shown to stabilize otherwise reactive ligands.[79] In **Figure 5c**, we present overlaid conductance histograms for **C10Br** and **C10Br-Me**, a molecular analogue in which α-hydrogens have been replaced by methyl groups. Both measurements provide a peak at the same conductance, indicating the formation of **CnBr** junctions does not involve α-hydride elimination processes resulting in carbenic contacts. We attribute the low intensity of the conductance feature in measurements of **C10Br-Me** (and 1,8-dibromoperfluorooctane (**C8Br-F**), **Figure 5f**) to the bulky groups proximal to the Br-C bond that may sterically inhibit junction formation or stability. To help maximize the histogram peak intensity, conductance measurements of **C10Br-Me** were performed after leaving the solution in contact with the substrate overnight.

In **Figure 5d**, we present overlaid conductance histograms for bitolyl-based junctions formed from 4,4′-bis((methylthio)methyl)biphenyl (**Tol2SMe**) and 4,4′-

bis(bromomethyl)biphenyl (**Tol2Br**), a molecule with no β-hydrogens. We use the conductance of **C10SMe** (**Figure 2a**) and **Tol2SMe** junctions as a point of reference to evaluate whether the junctions formed from **C10Br** (**Figure 2a**) and **Tol2Br** exhibit a markedly distinct or comparable contact chemistry (**Figure 5e**). We find that the peak conductance of **C10SMe** and **Tol2SMe** junctions is lower by a similar factor relative to the peak conductance of junctions formed from their Br-terminated analogues (by ×9.6 and ×3.5, respectively), implicating a similar contact chemistry. Notably, if the absence of β-hydrogens could stabilize a distinct, highly conducting C(sp^3)-Ag contact chemistry we would expect the conductance of junctions formed from **Tol2Br** to be orders of magnitude higher than the conductance of **Tol2SMe** junctions, given that the Ag-C bond would be both strongly coupled and well aligned with the backbone π-system (as shown for analogous junctions with gold electrodes).[40] Considering that **Tol2Br** cannot undergo β-hydride elimination reactions to form vinylic contacts, these results indicate that such processes also do not occur in **CnBr** junctions. As such, we conclude that this decomposition pathway is not responsible for the low contact conductance observed. In further support of this deduction, our attempts to directly measure alkene-terminated alkanes in junctions with silver electrodes have so far provided only inconsistent conductance features distinct to those shown here. Finally, in **Figure 5f**, we show that the conductance of junctions formed from **C8Br-F**, a molecule with no α- or β-hydrogens, is a factor of ~2 lower than that of **C8Br** junctions, providing additional supporting evidence that junctions formed from **CnBr** do not comprise significantly different carbenic or vinylic contacts. We propose that the slightly lower conductance of **C8Br-F** junctions may instead be attributed to the electron-withdrawing fluorine backbone substituents that are expected to impact level alignment between the conducting molecular orbital(s) and silver electrode E_F.[80]

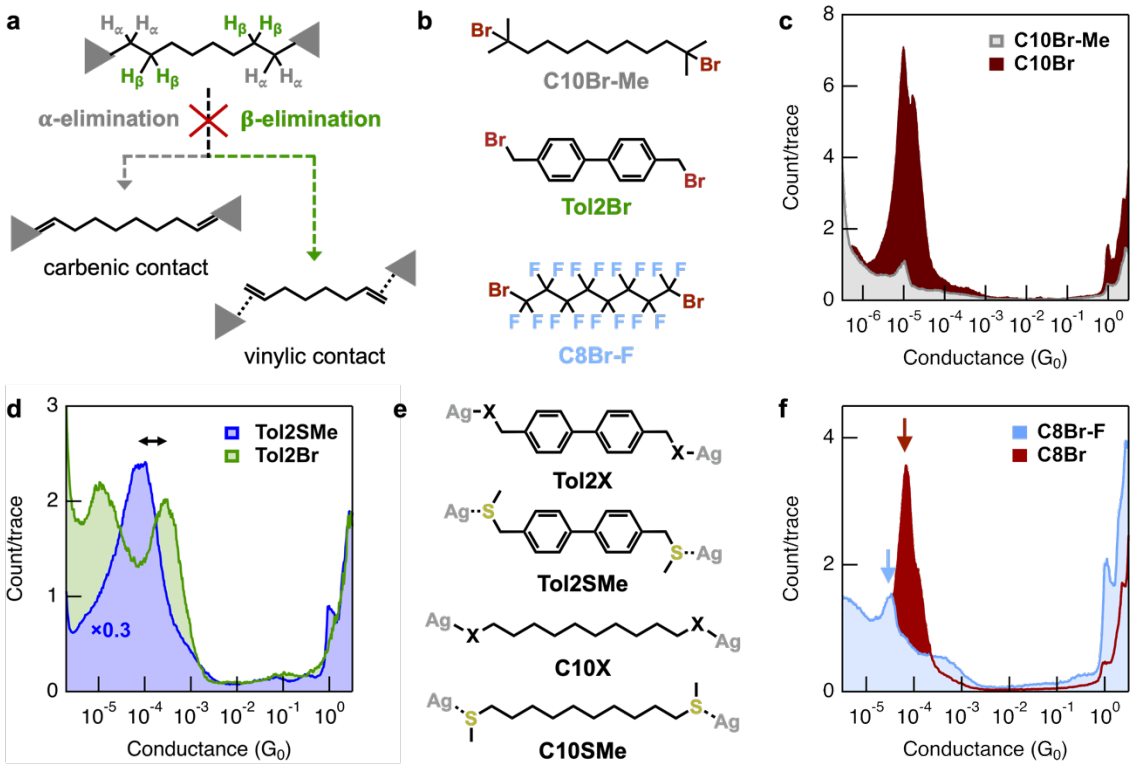

Figure 5. (a) Reaction scheme showing possible α- and β-hydride elimination processes to form junctions with carbenic or vinylic contacts. **(b)** Control molecules with substituents at α- (**C10Br-Me**), β- (**Tol2Br**), or both α- and β-positions (**C8Br-F**) that cannot readily undergo hydride elimination. **(c)** Overlaid 1D histograms of **C10Br-Me** (4,000 traces) and **C10Br** showing that each form junctions of similar conductance. This shows the formation of these junctions do not involve α-hydride elimination processes resulting in carbenic contacts. **(d)** Overlaid 1D histograms for bitolyl-based junctions formed from **Tol2Br** and **Tol2SMe** (peak separation indicated by black solid arrow). The junctions formed from bromide-terminated molecules exhibit a conductance that is higher by a similar ratio to alkane-based junctions formed from **C10Br** and **C10SMe** (**Figure 2a**; alkane: ×9.6, tolyl: ×3.5). These comparisons indicate we form junctions from **Tol2Br** that comprise a similar molecule-electrode contact chemistry as junctions formed from **C10Br**, and that this process does not involve β-hydride elimination reactions that result in vinylic contacts. We note that **Tol2Br** and **Tol2SMe** were measured in 1,2,4-trichlorobenzene solutions to facilitate their dissolution, and **Tol2Br** was measured at a concentration of 1 μM to facilitate the clean breaking of junctions. **(e)** Proposed schematic structures for the junctions formed in (d), illustrating their similarities. X = O for the alkoxide-terminated junctions proposed here based on prior temperature-programmed desorption studies and our transmission calculations. **(f)** Overlaid 1D histograms showing that the conductance of **C8Br-F** junctions is only a factor of ~2 lower than that of **C8Br** junctions. This suggests that these junctions exhibit similar contact chemistries, with conductance only influenced by backbone substituents that tune the energetic alignment of conducting orbitals with the silver E_F, further corroborating the studies using **C10Br-Me** and **Tol2Br**. Data for **CnBr** reproduced from **Figure 2a** for convenience.

CONCLUSION

Here we have demonstrated that alkyl halides uniquely and spontaneously form chemisorbed molecular junctions with silver electrodes, leveraging the ability of intrinsically reactive non-gold metal surfaces to activate otherwise inert functional molecular groups. Critically, however, we show that these junctions do not exhibit the high conductance expected for Ag-C(sp^3) linkages based on measurements of analogous precursors on gold, or from first-principles calculations based on DFT. We hypothesize that the most likely contact incorporates an insulating oxygen component through a multistep process that involves the reaction of an intermediate silver-alkyl species with surface adsorbed oxygen, resulting in the formation of Ag-O-C(sp^3) linkages. These findings expose fundamental challenges in transferring core concepts and methodologies in molecular electronics, established using model systems comprising gold electrodes, between different electrode materials with distinct properties.

More broadly, this work highlights the application of glovebox STM-BJ methods to perform molecular conductance measurements using air-sensitive metal electrodes to expose and characterize interfacial chemical reactions and charge transport. We anticipate that the established enhanced reactivity of simple, halide-functionalized molecules at silver and non-gold electrodes[62,81] will facilitate additional studies focused on the formation and evaluation of different M-C contact chemistries that build upon the approaches used here. In pursuing such experiments, we emphasize the value of exploring, integrating, and drawing inspiration from the wider surface science literature, which we recognize contains results and discussion of substantial relevance to the field of molecular electronics, but which have not yet been well-integrated into this field. Given the oxophilicity of many metals, we also propose that the development of new, robust approaches to form molecular junctions comprising metal-oxygen contacts will prove invaluable in evaluating the interfacial chemistry of chemisorbed species in junctions formed from non-gold electrodes.

ASSOCIATED CONTENT

Electronic Supplementary Information (ESI) available: Additional experimental details and synthetic methods, as well as conductance, computational, and spectroscopic data.

AUTHOR INFORMATION

Corresponding Author

Michael S. Inkpen – Email: inkpen@usc.edu

Héctor Vázquez – Email: vazquez@fzu.cz

Notes

The authors declare no competing financial interest.

ACKNOWLEDGEMENTS

This work was primarily supported by funding from the University of Southern California (USC), the National Science Foundation (NSF CAREER Award to M.S.I., CHE-2239614), and the Czech Science Foundation (GAČR) under project 23-05891S. N.R. was supported by a Marie Skłodowska Curie Global Fellowship (HOPELEC: 898657) within the Horizon 2020 Programme. Computational resources were supplied by the project "e-Infrastruktura CZ" (e-INFRA LM2018140) provided within the program Projects of Large Research, Development and Innovations Infrastructures. Instrumentation in the USC Chemistry Instrument Facility was acquired with support from the USC Research and Innovation Instrumentation Award Program. Additionally, funds provided by the NSF (DBI-0821671, CHE-0840366) and National Institute of Health (S10 RR25432) supported the acquisition of the NMR spectrometers used in our work.

REFERENCES

(1) Ulman, A. Formation and Structure of Self-Assembled Monolayers. *Chem. Rev.* **1996**, *96* (4), 1533–1554. https://doi.org/10.1021/cr9502357.
(2) Zhou, C.; Muller, C.; Burgin, T.; Tour, J.; Reed, M. Conductance of a Molecular Junction. *Science* **1997**, *278* (5336), 252–254.
(3) Xu, B.; Tao, N. J. Measurement of Single-Molecule Resistance by Repeated Formation of Molecular Junctions. *Science* **2003**, *301* (5637), 1221–1223.
(4) Su, T. A.; Neupane, M.; Steigerwald, M. L.; Venkataraman, L.; Nuckolls, C. Chemical Principles of Single-Molecule Electronics. *Nat. Rev. Mater.* **2016**, *1* (3), 16002. https://doi.org/10.1038/natrevmats.2016.2.
(5) Li, H.; Su, T.; Camarasa-Gómez, M.; Hernangómez-Pérez, D.; Henn, S.; Pokorný, V.; Caniglia, C. D.; Inkpen, M.; Korytár, R.; Steigerwald, M.; Nuckolls, C.; Evers, F.; Venkataraman, L. Silver Makes Better Electrical Contacts to Thiol-Terminated Silanes than Gold. *Angew. Chem. Int. Ed.* **2017**, *56* (45), 14145–14148. https://doi.org/10.1002/anie.201708524.
(6) Li, D. F.; Mao, J. C.; Chen, D. L.; Chen, F.; Ze-Wen, H.; Zhou, X. Y.; Wang, Y. H.; Zhou, X. S.; Niu, Z. J.; Maisonhaute, E. Single-Molecule Conductance with Nitrile and Amino Contacts with Ag or Cu Electrodes. *Electrochimica Acta* **2015**, *174*, 340–344. https://doi.org/10.1016/j.electacta.2015.06.018.
(7) Kim, H. S.; Kim, T. Dependence of the Conductance Change on the Molecular Orbitals in Ag and Au Electrodes. *J. Korean Phys. Soc.* **2016**, *68* (2), 279–282. https://doi.org/10.3938/jkps.68.279.
(8) Kim, T. Conductance of a Single Molecule Junction Formed with Ni, Au, and Ag Electrodes. *J. Korean Chem. Soc.* **2014**, *58* (6), 513–516. https://doi.org/10.5012/jkcs.2014.58.6.513.

(9) Kim, T.; Vázquez, H.; Hybertsen, M. S.; Venkataraman, L. Conductance of Molecular Junctions Formed with Silver Electrodes. *Nano Lett.* **2013**, *13* (7), 3358–3364. https://doi.org/10.1021/nl401654s.
(10) Kim, T. Substituent Effect on the Conductance of Single-Molecule Junctions Formed with Silver Electrodes. *J. Korean Phys. Soc.* **2015**, *67* (12), 2077–2080. https://doi.org/10.3938/jkps.67.2077.
(11) Adak, O.; Korytár, R.; Joe, A. Y.; Evers, F.; Venkataraman, L. Impact of Electrode Density of States on Transport through Pyridine-Linked Single Molecule Junctions. *Nano Lett.* **2015**, *15* (6), 3716–3722. https://doi.org/10.1021/acs.nanolett.5b01195.
(12) Zhou, X. Y.; Wang, Y. H.; Qi, H. M.; Zheng, J. F.; Niu, Z. J.; Zhou, X. S. Single-Molecule Conductance of Dipyridines Binding to Ag Electrodes Measured by Electrochemical Scanning Tunneling Microscopy Break Junction. *Nanoscale Res. Lett.* **2014**, *9* (1), 1–6. https://doi.org/10.1186/1556-276X-9-77.
(13) Li, S.; Yu, H.; Chen, X.; Gewirth, A. A.; Moore, J. S.; Schroeder, C. M. Covalent Ag-C Bonding Contacts from Unprotected Terminal Acetylenes for Molecular Junctions. *Nano Lett.* **2020**, *20* (7), 5490–5495. https://doi.org/10.1021/acs.nanolett.0c02015.
(14) Song, K.; Lin, J.; Song, X.; Yang, B.; Zhu, J.; Zang, Y.; Zhu, D. Formation of Covalent Metal–Carbon Contacts Assisted by Ag+ for Single Molecule Junctions. **2023**. https://doi.org/10.1039/d3cc01113e.
(15) Song, K.; Lin, J.; Song, X.; Zhang, M.; Gu, Q.; Zang, Y.; Zhu, D. In Situ Creation of Organometallic Molecular Junctions via Terminal Alkynes. *J Phys Chem C* **2023**, *127* (18), 8850. https://doi.org/10.1021/acs.jpcc.3c01337.
(16) Zhou, X. S.; Liang, J. H.; Chen, Z. Bin; Mao, B. W. An Electrochemical Jump-to-Contact STM-Break Junction Approach to Construct Single Molecular Junctions with Different Metallic Electrodes. *Electrochem. Commun.* **2011**, *13* (5), 407–410. https://doi.org/10.1016/j.elecom.2011.02.005.
(17) Wang, Y. H.; Hong, Z. W.; Sun, Y. Y.; Li, D. F.; Han, D.; Zheng, J. F.; Niu, Z. J.; Zhou, X. S. Tunneling Decay Constant of Alkanedicarboxylic Acids: Different Dependence on the Metal Electrodes between Air and Electrochemistry. *J. Phys. Chem. C* **2014**, *118* (32), 18756–18761. https://doi.org/10.1021/jp505374v.
(18) Peng, Z. L.; Chen, Z. Bin; Zhou, X. Y.; Sun, Y. Y.; Liang, J. H.; Niu, Z. J.; Zhou, X. S.; Mao, B. W. Single Molecule Conductance of Carboxylic Acids Contacting Ag and Cu Electrodes. *J. Phys. Chem. C* **2012**, *116* (41), 21699–21705. https://doi.org/10.1021/jp3069046.
(19) Engelkes, V. B.; Beebe, J. M.; Frisbie, C. D. Length-Dependent Transport in Molecular Junctions Based on SAMs of Alkanethiols and Alkanedithiols: Effect of Metal Work Function and Applied Bias on Tunneling Efficiency and Contact Resistance. *J. Am. Chem. Soc.* **2004**, *126* (43), 14287–14296. https://doi.org/10.1021/ja046274u.
(20) Kim, B.; Choi, S. H.; Zhu, X. Y.; Frisbie, C. D. Molecular Tunnel Junctions Based on π-Conjugated Oligoacene Thiols and Dithiols between Ag, Au, and Pt Contacts: Effect of Surface Linking Group and Metal Work Function. *J Am Chem Soc* **2011**, *133* (49), 19864–19877. https://doi.org/10.1021/ja207751w.
(21) Wang, J. G.; Prodan, E.; Car, R.; Selloni, A. Band Alignment in Molecular Devices: Influence of Anchoring Group and Metal Work Function. *Phys. Rev. B - Condens. Matter Mater. Phys.* **2008**, *77* (24), 1–8. https://doi.org/10.1103/PhysRevB.77.245443.
(22) Adak, O.; Korytár, R.; Joe, A. Y.; Evers, F.; Venkataraman, L. Impact of Electrode Density of States on Transport through Pyridine-Linked Single Molecule Junctions. *Nano Lett.* **2015**, *15* (6), 3716–3722. https://doi.org/10.1021/acs.nanolett.5b01195.
(23) Cheng, Z. L.; Skouta, R.; Vazquez, H.; Widawsky, J. R.; Schneebeli, S.; Chen, W.; Hybertsen, M. S.; Breslow, R.; Venkataraman, L. In Situ Formation of Highly

Conducting Covalent Au-C Contacts for Single-Molecule Junctions. *Nat Nanotechnol* **2011**, *6* (6), 353–357. http://www.nature.com/nnano/journal/v6/n6/abs/nnano.2011.66.html#supplementary-information.

(24) Park, Y. S.; Whalley, A. C.; Kamenetska, M.; Steigerwald, M. L.; Hybertsen, M. S.; Nuckolls, C.; Venkataraman, L. Contact Chemistry and Single-Molecule Conductance: A Comparison of Phosphines, Methyl Sulfides, and Amines. *J Am Chem Soc* **2007**, *129* (51), 15768–15769. https://doi.org/10.1021/ja0773857.

(25) Frei, M.; Aradhya, S. V.; Hybertsen, M. S.; Venkataraman, L. Linker Dependent Bond Rupture Force Measurements in Single-Molecule Junctions. *J Am Chem Soc* **2012**, *134* (9), 4003–4006. https://doi.org/10.1021/ja211590d.

(26) Quek, S. Y.; Kamenetska, M.; Steigerwald, M. L.; Choi, H. J.; Louie, S. G.; Hybertsen, M. S.; Neaton, J. B.; Venkataraman, L. Mechanically Controlled Binary Conductance Switching of a Single-Molecule Junction. *Nat. Nanotechnol.* **2009**, *4* (4), 230–234. https://doi.org/10.1038/nnano.2009.10.

(27) Zhou, Q.; Song, K.; Zhang, G.; Song, X.; Lin, J.; Zang, Y.; Zhang, D.; Zhu, D. Tetrathiafulvalenes as Anchors for Building Highly Conductive and Mechanically Tunable Molecular Junctions. *Nat. Commun.* **2022**, *13* (1), 1–8. https://doi.org/10.1038/s41467-022-29483-2.

(28) Jo, H. Y.; Yoo, P. S.; Kim, T. Oxygen-Silver Junction Formation for Single Molecule Conductance. *J. Korean Chem. Soc.* **2015**, *59* (1), 18–21. https://doi.org/10.5012/jkcs.2015.59.1.18.

(29) Lortscher, E. Wiring Molecules into Circuits. *Nat Nanotechnol* **2013**, *8* (6), 381–384. https://doi.org/10.1038/nnano.2013.105.

(30) Stone, I.; Starr, R. L.; Zang, Y.; Nuckolls, C.; Steigerwald, M. L.; Lambert, T. H.; Roy, X.; Venkataraman, L. A Single-Molecule Blueprint for Synthesis. *Nat. Rev. Chem.* **2021**, *5*, 695–710. https://doi.org/10.1038/s41570-021-00316-y.

(31) Lindner, R.; Kühnle, A. On-Surface Reactions. *ChemPhysChem* **2015**, *16* (8), 1582–1592. https://doi.org/10.1002/cphc.201500161.

(32) Hannagan, R. T.; Giannakakis, G.; Flytzani-Stephanopoulos, M.; Sykes, E. C. H. Single-Atom Alloy Catalysis. *Chem. Rev.* **2020**, *120* (21), 12044–12088. https://doi.org/10.1021/acs.chemrev.0c00078.

(33) Xiang, L.; Hines, T.; Palma, J. L.; Lu, X.; Mujica, V.; Ratner, M. A.; Zhou, G.; Tao, N. Non-Exponential Length Dependence of Conductance in Iodide-Terminated Oligothiophene Single-Molecule Tunneling Junctions. *J Am Chem Soc* **2016**, *138*, 679–687.

(34) Peng, L. L.; Huang, B.; Zou, Q.; Hong, Z. W.; Zheng, J. F.; Shao, Y.; Niu, Z. J.; Zhou, X. S.; Xie, H. J.; Chen, W. Low Tunneling Decay of Iodine-Terminated Alkane Single-Molecule Junctions. *Nanoscale Res. Lett.* **2018**, *13*. https://doi.org/10.1186/s11671-018-2528-z.

(35) Komoto, Y.; Fujii, S.; Hara, K.; Kiguchi, M. Single Molecular Bridging of Au Nanogap Using Aryl Halide Molecules. *J. Phys. Chem. C* **2013**, *117* (46), 24277–24282. https://doi.org/10.1021/jp404858x.

(36) Starr, R. L.; Fu, T.; Doud, E. A.; Stone, I.; Roy, X.; Venkataraman, L. Gold–Carbon Contacts from Oxidative Addition of Aryl Iodides. *J. Am. Chem. Soc.* **2020**, *142* (15), 7128–7133. https://doi.org/10.1021/jacs.0c01466.

(37) Stone, I. B.; Starr, R. L.; Hoffmann, N.; Wang, X.; Evans, A. M.; Nuckolls, C.; Lambert, T. H.; Steigerwald, M. L.; Berkelbach, T. C.; Roy, X.; Venkataraman, L. Interfacial Electric Fields Catalyze Ullmann Coupling Reactions on Gold Surfaces. *Chem. Sci.* **2022**, 20–24. https://doi.org/10.1039/d2sc03780g.

(38) Li, Y.; Buerkle, M.; Li, G.; Rostamian, A.; Wang, H.; Wang, Z.; Bowler, D. R.; Miyazaki, T.; Xiang, L.; Asai, Y.; Zhou, G.; Tao, N. Gate Controlling of Quantum Interference and Direct Observation of Anti-Resonances in Single Molecule Charge Transport. *Nat. Mater.* **2019**, *18* (4), 357–363. https://doi.org/10.1038/s41563-018-0280-5.
(39) Wei, C.; Ye, J.; Su, Y.; Zheng, J.; Xiao, S.; Chen, J.; Yuan, S.; Zhang, C.; Bai, J. Halide Anchors for Single-Cluster Electronics. *CCS Chem.* **2022**, *5*, 1–9. https://doi.org/10.31635/ccschem.022.202202180.
(40) Chen, W.; Widawsky, J. R.; Vázquez, H.; Schneebeli, S. T.; Hybertsen, M. S.; Breslow, R.; Venkataraman, L. Highly Conducting π-Conjugated Molecular Junctions Covalently Bonded to Gold Electrodes. *J. Am. Chem. Soc.* **2011**, *133* (43), 17160–17163. https://doi.org/10.1021/ja208020j.
(41) Miyaura, N.; Suzuki, A. Palladium-Catalyzed Cross-Coupling Reactions of Organoboron Compounds. *Chem Rev* **1995**, *95* (7), 2457–2483. https://doi.org/10.1021/cr00039a007.
(42) Sambiagio, C.; Marsden, S. P.; Blacker, A. J.; McGowan, P. C. Copper Catalysed Ullmann Type Chemistry: From Mechanistic Aspects to Modern Development. *Chem Soc Rev* **2014**, *43* (10), 3525–3550. https://doi.org/10.1039/c3cs60289c.
(43) Ariafard, A.; Lin, Z. Understanding the Relative Easiness of Oxidative Addition of Aryl and Alkyl Halides to Palladium(0). *Organometallics* **2006**, *25* (16), 4030–4033. https://doi.org/10.1021/om060236x.
(44) Sorenson, S. A.; Patrow, J. G.; Dawlaty, J. M. Solvation Reaction Field at the Interface Measured by Vibrational Sum Frequency Generation Spectroscopy. *J. Am. Chem. Soc.* **2017**, *139* (6), 2369–2378. https://doi.org/10.1021/jacs.6b11940.
(45) Livendahl, M.; Espinet, P.; Echavarren, A. M. Final Analysis: Is Gold a Catalyst in Cross-Coupling Reactions in the Absence of Palladium? *Platin. Met. Rev.* **2011**, *55* (3), 212–214. https://doi.org/10.1595/147106711X579128.
(46) Björk, J.; Hanke, F.; Stafström, S. Mechanisms of Halogen-Based Covalent Self-Assembly on Metal Surfaces. *J. Am. Chem. Soc.* **2013**, *135* (15), 5768–5775. https://doi.org/10.1021/ja400304b.
(47) Doud, E. A.; Inkpen, M. S.; Lovat, G.; Montes, E.; Paley, D. W.; Steigerwald, M. L.; Vázquez, H.; Venkataraman, L.; Roy, X. In Situ Formation of N-Heterocyclic Carbene-Bound Single-Molecule Junctions. *J. Am. Chem. Soc.* **2018**, *140* (28), 8944–8949. https://doi.org/10.1021/jacs.8b05184.
(48) Jones, G. S.; Barteau, M. A.; Vohs, J. M. Mechanism of Diethyl Ether Formation on Ag(110) and Its Dependence on Coadsorbed Oxygen Species. *J. Phys. Chem. B* **1999**, *103* (7), 1144–1151. https://doi.org/10.1021/jp983997p.
(49) Jones, G. S.; Barteau, M. A.; Vohs, J. M. The Formation of Diethyl Ether via the Reaction of Iodoethane with Atomic Oxygen on the Ag(110) Surface. *Surf. Sci.* **1999**, *420* (1), 65–80. https://doi.org/10.1016/S0039-6028(98)00821-8.
(50) Zhou, X.-L.; Solymosi, F.; Blass, P. M.; Cannon, K. C.; White, J. M. Interactions of Methyl Halides (Cl, Br and I) with Ag(111). *Surf. Sci.* **1989**, *219*, 294–316.
(51) Zhou, X.-L.; White, J. M. Thermal Decomposition of C2H5I on Ag(111). *Catal. Lett.* **1989**, *2*, 375–384.
(52) Venkataraman, L.; Klare, J. E.; Tam, I. W.; Nuckolls, C.; Hybertsen, M. S.; Steigerwald, M. L. Single-Molecule Circuits with Well-Defined Molecular Conductance. *Nano Lett* **2006**, *6* (3), 458–462. https://doi.org/10.1021/nl052373+.
(53) Miao, Z.; Quainoo, T.; Czyszczon-Burton, T. M.; Rotthowe, N.; Parr, J. M.; Liu, Z.; Inkpen, M. S. Charge Transport across Dynamic Covalent Chemical Bridges. *Nano Lett* **2022**, *22* (20), 8331–8338. https://doi.org/10.1021/acs.nanolett.2c03288.

(54) Kim, T.; Vázquez, H.; Hybertsen, M. S.; Venkataraman, L. Conductance of Molecular Junctions Formed with Silver Electrodes. *Nano Lett.* **2013**, *13* (7), 3358–3364. https://doi.org/10.1021/nl401654s.
(55) Smit, R. H. M.; Untiedt, C.; Yanson, A. I.; Van Ruitenbeek, J. M. Common Origin for Surface Reconstruction and the Formation of Chains of Metal Atoms. *Phys. Rev. Lett.* **2001**, *87* (26), 266102-1-266102–266104. https://doi.org/10.1103/PhysRevLett.87.266102.
(56) Kim, T. Silver Electrodes for Reversible Oxygen Sensor Applications. *J. Korean Phys. Soc.* **2015**, *67* (5), 823–826. https://doi.org/10.3938/jkps.67.823.
(57) Reuter, M. G.; Solomon, G. C.; Hansen, T.; Seideman, T.; Ratner, M. A. Understanding and Controlling Crosstalk between Parallel Molecular Wires. *J. Phys. Chem. Lett.* **2011**, *2* (14), 1667–1671. https://doi.org/10.1021/jz200658h.
(58) Obersteiner, V.; Egger, D. A.; Zojer, E. Impact of Anchoring Groups on Ballistic Transport: Single Molecule vs Monolayer Junctions. *J. Phys. Chem. C* **2015**, *119* (36), 21198–21208. https://doi.org/10.1021/acs.jpcc.5b06110.
(59) Capozzi, B.; Low, J. Z.; Xia, J.; Liu, Z.-F.; Neaton, J. B.; Campos, L. M.; Venkataraman, L. Mapping the Transmission Functions of Single-Molecule Junctions. *Nano Lett.* **2016**, *16* (6), 3949–3954. https://doi.org/10.1021/acs.nanolett.6b01592.
(60) Leary, E.; Zotti, L. A.; Miguel, D.; Márquez, I. R.; Palomino-Ruiz, L.; Cuerva, J. M.; Rubio-Bollinger, G.; González, M. T.; Agrait, N. The Role of Oligomeric Gold–Thiolate Units in Single-Molecule Junctions of Thiol-Anchored Molecules. *J. Phys. Chem. C* **2018**, *122* (6), 3211–3218. https://doi.org/10.1021/acs.jpcc.7b11104.
(61) Inkpen, M. S.; Liu, Z.; Li, H.; Campos, L. M.; Neaton, J. B.; Venkataraman, L. Non-Chemisorbed Gold–Sulfur Binding Prevails in Self-Assembled Monolayers. *Nat. Chem.* **2019**, *11*, 351–358.
(62) Zaera, F. The Surface Chemistry of Hydrocarbon Fragments on Transition Metals: Towards Understanding Catalytic Processes. *Mol. Phys.* **2002**, *100* (19), 3065–3073. https://doi.org/10.1080/00268970210130254.
(63) Zhou, X. L.; White, J. M. Reactions of Iodoethane, Iodopropane, 2-Iodopropane, Chloroiodomethane Adsorbed on Silver(111). *J. Phys. Chem.* **1991**, *95* (14), 5575–5580. https://doi.org/10.1021/j100167a039.
(64) Whitesides, G. M.; Bergbreiter, D. E.; Kendall, P. E. Preparation and Thermal Decomposition of N-Alkyl(Tri-n-Butylphosphine)Silver(I) Reagents. *J. Am. Chem. Soc.* **1974**, *96* (9), 2806–2813. https://doi.org/10.1021/ja00816a024.
(65) Porter, K. A.; Schier, A.; Schmidbaur, H. α,ω-Bis[(Triphenylphosphine)Gold(I)] Hydrocarbons. In *Perspectives in Organometallic Chemistry*; 2003.
(66) Zotti, L. A.; Bürkle, M.; Pauly, F.; Lee, W.; Kim, K.; Jeong, W.; Asai, Y.; Reddy, P.; Cuevas, J. C. Heat Dissipation and Its Relation to Thermopower in Single-Molecule Junctions. *New J. Phys.* **2014**, *16* (1), 015004. https://doi.org/10.1088/1367-2630/16/1/015004.
(67) Quek, S. Y.; Venkataraman, L.; Choi, H. J.; Louie, S. G.; Hybertsen, M. S.; Neaton, J. B. Amine−Gold Linked Single-Molecule Circuits: Experiment and Theory. *Nano Lett* **2007**, *7* (11), 3477–3482. https://doi.org/10.1021/nl072058i.
(68) Markussen, T.; Jin, C.; Thygesen, K. S. Quantitatively Accurate Calculations of Conductance and Thermopower of Molecular Junctions. *Phys. Status Solidi B* **2013**, *250* (11), 2394–2402. https://doi.org/10.1002/pssb.201349217.
(69) Refaely-Abramson, S.; Liu, Z.-F.; Bruneval, F.; Neaton, J. B. First-Principles Approach to the Conductance of Covalently Bound Molecular Junctions. *J. Phys. Chem. C* **2019**, *123* (11), 6379–6387. https://doi.org/10.1021/acs.jpcc.8b12124.

(70) Montes, E.; Vázquez, H. Calculation of Energy Level Alignment and Interface Electronic Structure in Molecular Junctions beyond DFT. *J. Phys. Chem. C* **2021**, *125* (46), 25825–25831. https://doi.org/10.1021/acs.jpcc.1c07407.
(71) Fatemi, V.; Kamenetska, M.; Neaton, J. B.; Venkataraman, L. Environmental Control of Single-Molecule Junction Transport. *Nano Lett.* **2011**, *11* (5), 1988–1992. https://doi.org/10.1021/nl200324e.
(72) Weiss, E. A.; Kaufman, G. K.; Kriebel, J. K.; Li, Z.; Schalek, R.; Whitesides, G. M. Si/SiO2-Templated Formation of Ultraflat Metal Surfaces on Glass, Polymer, and Solder Supports: Their Use as Substrates for Self-Assembled Monolayers. *Langmuir* **2007**, *23* (19), 9686–9694. https://doi.org/10.1021/la701919r.
(73) Backx, C.; de Groot, C. P. M.; Biloen, P. ADSORPTION OF OXYGEN ON Ag(110) STUDIED BY HIGH RESOLUTION ELS AND TPD. *Surf. Sci.* **1981**, *104*, 300–317.
(74) Wachs, I. E.; Madix, R. J. The Oxidation of Methanol on a Silver (110) Catalyst. *Surf. Sci.* **1978**, *76* (2), 531–558. https://doi.org/10.1016/0039-6028(78)90113-9.
(75) Lawson, B.; Skipper, H. E.; Kamenetska, M. Phenol Is a pH-Activated Linker to Gold: A Single Molecule Conductance Study. *Nanoscale* **2024**, *16* (4), 2022–2029. https://doi.org/10.1039/D3NR05257E.
(76) Li, W.-X.; Stampfl, C.; Scheffler, M. Oxygen Adsorption on Ag(111): A Density-Functional Theory Investigation. *Phys. Rev. B* **2002**, *65* (7), 075407. https://doi.org/10.1103/PhysRevB.65.075407.
(77) Zaera, F. The Surface Chemistry of Hydrocarbons on Transition Metal Surfaces: A Critical Review. *Isr. J. Chem.* **1998**, *38* (4), 293–311. https://doi.org/10.1002/ijch.199800035.
(78) Schrock, R. R. Alkylidene Complexes of Niobium and Tantalum. *Acc. Chem. Res.* **1979**, *12* (3), 98–104. https://doi.org/10.1021/ar50135a004.
(79) Mowat, W.; Shortland, A.; Yagupsky, G.; Hill, N. J.; Yagupsky, M.; Wilkinson, G. Elimination Stabilized Alkyls. Part I. Chromium, Molybdenum, Tungsten, and Vanadium. *J Chem Soc Dalton Trans* **1972**, 533–542.
(80) Venkataraman, L.; Park, Y. S.; Whalley, A. C.; Nuckolls, C.; Hybertsen, M. S.; Steigerwald, M. L. Electronics and Chemistry: Varying Single-Molecule Junction Conductance Using Chemical Substituents. *Nano Lett.* **2007**, *7* (2), 502–506. https://doi.org/10.1021/nl062923j.
(81) Zaera, F. Preparation and Reactivity of Alkyl Groups Adsorbed on Metal Surfaces. *Acc. Chem. Res.* **1992**, *25* (6), 260–265. https://doi.org/10.1021/ar00018a003.